Available online at www.sciencedirect.com
SCIENCE DIRECT®
Advances in Space Research 33 (2004) 537–541
ADVANCES IN SPACE RESEARCH
(a COSPAR publication)
www.elsevier.com/locate/asr

Atmospheres of magnetized neutron stars: vacuum polarization and partially ionized models

Wynn C.G. Ho [a,*], Dong Lai [a], Alexander Y. Potekhin [b], Gilles Chabrier [c]

[a] *Center for Radiophysics and Space Research, Department of Astronomy, Cornell University, Ithaca, NY 14853, USA*
[b] *Ioffe Physico-Technical Institute, Politekhnicheskaya 26, 194021, St. Petersburg, Russia*
[c] *CRAL (UMR CNRS No. 5574), Ecole Normale Supérieure de Lyon, 69364 Lyon Cedex 07, France*

Received 27 November 2002; received in revised form 15 February 2003; accepted 15 February 2003

Abstract

We construct hydrogen atmospheric models for magnetized neutron stars (NSs) in radiative equilibrium with surface fields $B = 10^{12}$–5×10^{14} G and effective temperatures $T_{\rm eff} \sim$ a few $\times\, 10^5$–10^6 K by solving the full radiative transfer equations for both polarization modes in the magnetized hydrogen plasma. The atmospheres directly determine the characteristics of thermal emission from isolated NSs. We study the effects of vacuum polarization and bound atoms on the atmosphere structure and spectra. For the lower magnetic field models ($B \sim 10^{12}$ G), the spectral features due to neutral atoms lie at extreme UV and very soft X-ray energies and therefore are not likely to be observed. However, the continuum flux is also different from the fully ionized case, especially at lower energies. For the higher magnetic field models, we find that vacuum polarization softens the high energy tail of the thermal spectrum. We show that this depression of continuum flux strongly suppresses not only the proton cyclotron line but also spectral features due to bound species; therefore, spectral lines or features in thermal radiation are more difficult to observe when the NS magnetic field is $\gtrsim 10^{14}$ G.

Keywords: Atmospheres of magnetized neutron stars; Vacuum polarization; Partially ionized models; Atmospheric models

1. Introduction

Thermal radiation from the surface of isolated neutron stars (NSs) can provide invaluable information on the physical properties and evolution of NSs. Such radiation has been detected in various types of isolated NSs: from radio pulsars (see Becker, 2000; Pavlov et al., 2002) to old and young radio-quiet NSs (see Treves et al., 2000; Pavlov et al., 2002) to soft gamma-ray repeaters (SGRs) and anomalous X-ray pulsars (AXPs) (see Hurley, 2000; Israel et al., 2002; Mereghetti et al., 2002), which form a potentially new class of NSs ("magnetars") endowed with superstrong ($B \gtrsim 10^{14}$ G) magnetic fields (see Thompson and Duncan, 1996; Thompson, 2001). The NS surface emission is mediated by the thin atmospheric layer (with scale height ~0.1–10 cm and density ~0.1–100 g/cm^3) that covers the stellar surface. Therefore, to properly interpret the observations of NS surface emission and to provide accurate constraints on the physical properties of NSs, it is important to understand in detail the radiative properties of NS atmospheres in the presence of strong magnetic fields.

Steady progress has been made over the years in modeling NS atmospheres (see Pavlov et al., 1995; Ho and Lai, 2001, 2003; Zavlin and Pavlov, 2002 for more detailed references on observations and on previous works of NS atmosphere modeling). These atmospheric models have played a valuable role in assessing the observed spectra of radio pulsars and radio-quiet NSs. We have studied the H and He atmospheres of NSs with magnetic fields $B \sim 10^{12}$–10^{15} G and effective temperatures $T_{\rm eff} \sim 10^5$–10^7 K (Ho and Lai, 2001, 2003; Ho et al., 2003). Here we briefly discuss our atmospheric

* Corresponding author. Tel.: +1-650-926-2693; fax: +1-650-926-2221.
E-mail address: wynnho@astro.cornell.edu (W.C.G. Ho).

0273-1177/$30 © 2003 COSPAR. Published by Elsevier Ltd. All rights reserved.
doi:10.1016/j.asr.2003.02.016

model and the effects of vacuum polarization and report on recent work in incorporating hydrogen bound species in the models to produce partially ionized atmospheres.

2. Atmospheric model

We consider an isolated NS with a plane-parallel atmosphere. This is justified since the atmospheric scale height $H \lesssim 10$ cm is much less than the NS radius $R \approx 10$ km. The atmosphere is composed of pure hydrogen. A uniform magnetic field $\mathbf{B}$, aligned perpendicular to the surface, permeates the atmosphere, and the spectra presented indicate emission from a local patch of the NS surface with the indicated magnetic field strength and effective temperature.

In the highly magnetized plasma that characterizes NS atmospheres, there are two photon polarization modes, and they have very different radiative opacities. The two photon modes are the extraordinary mode (X-mode), which is mostly polarized perpendicular to the $\hat{\mathbf{k}}$–$\hat{\mathbf{B}}$ plane, and the ordinary mode (O-mode), which is mostly polarized parallel to the $\hat{\mathbf{k}}$–$\hat{\mathbf{B}}$ plane, where $\hat{\mathbf{k}}$ specifies the direction of photon propagation and $\hat{\mathbf{B}}$ is the direction of the external magnetic field. The O-mode has a significant component of its electric field $\mathbf{E}$ along $\hat{\mathbf{B}}$ for most directions of propagation, except when $\hat{\mathbf{k}}$ is nearly parallel to $\hat{\mathbf{B}}$, and therefore the O-mode opacity is close to the $B = 0$ value, while the X-mode opacity is much smaller.

To construct self-consistent atmospheric models requires successive iterations, where the temperature profile $T(\tau)$ is adjusted from the previous iteration in order to satisfy radiative equilibrium (τ is the Thomson depth within the atmosphere). We solve the radiative transfer equations (RTEs) for the two coupled photon polarization modes, together with the boundary conditions, by the finite difference scheme described in Mihalas (1978). We use a variation of the Unsold–Lucy temperature correction method as described in Mihalas (1978) but modified to account for full radiative transfer by two propagation modes in a magnetic medium. The process of determining the radiation intensity from the RTE for a given temperature profile, estimating and applying the temperature correction, and then recalculating the radiation intensity is repeated until convergence of the solution is achieved (see Ho and Lai, 2001 for details of our numerical method).

3. Vacuum polarization

It is well known that polarization of the vacuum due to virtual e^+e^- pairs becomes significant when $B \gtrsim B_Q$, where $B_Q = m_e^2c^3/e\hbar = 4.414 \times 10^{13}$ G. Vacuum polarization modifies the dielectric property of the medium and the polarization of photon modes, thereby altering the radiative scattering and absorption opacities (see Ho and Lai, 2003 and references therein). Of particular interest is the "vacuum resonance" phenomenon, which occurs when the effects of the vacuum and plasma on the linear polarization of the modes cancel each other, giving rise to a resonance feature in the opacity at photon energy $E_V \approx 1.02(Z/A)(\rho/1\ \mathrm{g\,cm^{-3}})^{1/2}(B/10^{14}\ \mathrm{G})^{-1}f(B)$ keV, where Z and A are the atomic charge and mass of the ion, respectively, ρ is the density, and $f(B)$ is a slowly-varying function of B of order unity.

It was shown in Lai and Ho (2002, 2003) (see also Gnedin et al., 1978; Pavlov and Gnedin, 1984) that high energy photons propagating in the atmospheric plasma can adiabatically convert from one polarization mode into another at the vacuum resonance density $\rho_V \approx 0.96(A/Z)(E/1\ \mathrm{keV})^2(B/10^{14}\ \mathrm{G})^2 f(B)^{-2}\ \mathrm{g\,cm^{-3}}$. Across the resonance, the orientation of the polarization ellipse rotates by 90°, although the helicity does not change (see Fig. 1). This resonant mode conversion is analogous to the Mikheyev–Smirnov–Wolfenstein (MSW) effect for neutrino oscillations. Because the two photon modes have vastly different opacities, this vacuum-induced mode conversion can significantly affect radiative transfer in strongly magnetized atmospheres. Fig. 2 illustrates the main effect that vacuum polarization has on the atmospheric spectrum. The left side of Fig. 2 shows the decoupling densities of the O-mode and X-mode photons (i.e., the densities of their respective photospheres) when the vacuum polarization effect is neglected. The right side of Fig. 2 shows that the effective decoupling depths of the photons are changed when the vacuum resonance lies between these two photospheres. We see from Fig. 2 that mode conversion makes the effective decoupling density of X-mode photons (which carry the bulk of the thermal energy) smaller, thereby

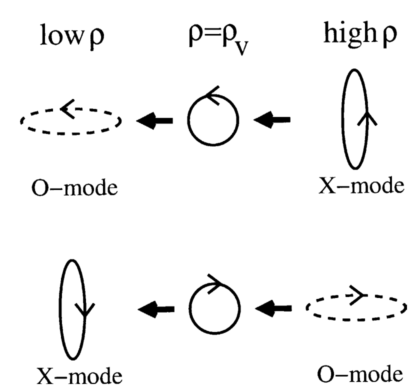

Fig. 1. A schematic diagram illustrating mode conversion due to vacuum polarization: as an X-mode (O-mode) photon at high density traverses the vacuum resonance density ρ_V, it becomes an O-mode (X-mode) photon at low density if the adiabatic condition is satisfied. In this evolution, the polarization ellipse rotates 90°, and the photon opacity changes significantly.

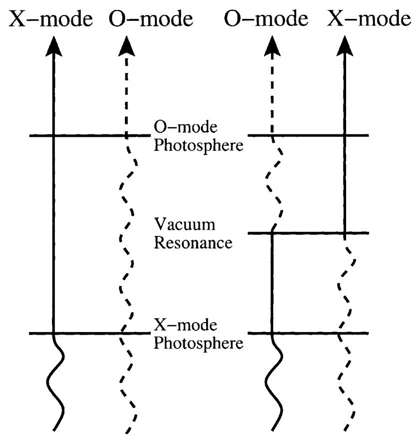

Fig. 2. A schematic diagram illustrating how vacuum polarization-induced mode conversion affects radiative transfer in a magnetar atmosphere. When the vacuum polarization effect is turned off, the X-mode photosphere (where optical depth ∼1) lies deeper than the O-mode. With the vacuum polarization effect included, the X-mode effectively decouples (emerges) from the atmosphere at the vacuum resonance, which lies at a lower density than the (original) X-mode photosphere.

depleting the high energy tail of the spectrum and making the spectrum closer to blackbody (although the spectrum is still harder than blackbody because of non-grey opacities). This expectation is borne out in self-consistent atmosphere modeling presented in Ho and Lai (2003) and illustrated in Fig. 3 for the case of $B = 5 \times 10^{14}$ G and $T_{\rm eff} = 5 \times 10^{6}$ K (all the models presented here use the corrected free-free absorption, which properly accounts for electron-ion collisions; Potekhin and Chabrier, 2003; see also Ho et al., 2003).

Another important effect of vacuum polarization on the spectrum, first noted in Ho and Lai (2003) and illustrated in Fig. 3, is the suppression of proton cyclotron lines (and other spectral lines; see below). The physical origin for such line suppression is related to the depletion of continuum flux; this depletion makes the decoupling depths inside and outside the line similar.

4. Partially ionized atmospheres

A major complication when incorporating bound species in the atmospheric models arises from the strong coupling between the center-of-mass motion of the atom and the internal atomic structure. Potekhin and Chabrier (2003) have constructed the first thermodynamically consistent equation of state and opacity models of partially ionized hydrogen plasmas in strong magnetic fields. From the work of Potekhin and Chabrier (2003), we obtain tables for the equation of state and absorption opacities of hydrogen, including the bound states. We interpolate between the table values to obtain densities and absorption opacities corresponding to the numerical grid of our models. (Note that we calculate the polarization vector of the medium assuming the medium is fully ionized since the abundance of bound species is very low for the cases considered; this is not strictly correct; see Bulik and Pavlov (1996) for the case where the atmosphere is completely neutral.) Thus we are able to obtain partially ionized hydrogen atmospheric models (Ho et al., 2003).

Fig. 4 shows the spectra of hydrogen atmospheres with $B = 10^{12}$ G and $T_{\rm eff} = 5 \times 10^{5}$ K, along with the non-magnetic hydrogen atmospheric model at the same $T_{\rm eff}$ and the blackbody spectrum with $T = 5 \times 10^{5}$ K. The proton cyclotron line at 6.3 eV is clear in both the fully ionized and partially ionized spectra. (The width of the proton cyclotron line in all the partially ionized

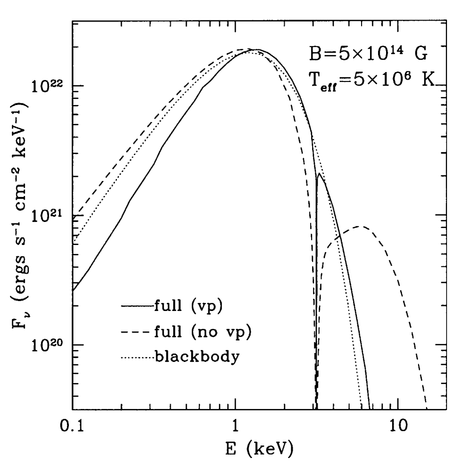

Fig. 3. Spectra of fully ionized hydrogen atmospheres with $B = 5 \times 10^{14}$ G and $T_{\rm eff} = 5 \times 10^{6}$ K. The solid line is for an atmosphere which includes vacuum polarization, the dashed line is for an atmosphere which neglects vacuum polarization, and the dotted line is for a blackbody with $T = 5 \times 10^{6}$ K.

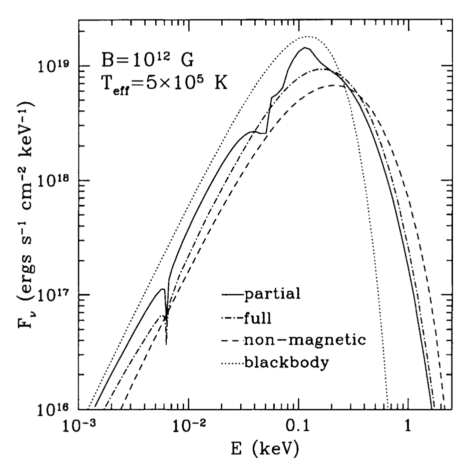

Fig. 4. Spectra of hydrogen atmospheres with $B = 10^{12}$ G and $T_{\rm eff} = 5 \times 10^{5}$ K. The solid line is for a partially ionized atmosphere, the dot-dashed line is for a fully ionized atmosphere, the dashed line is for a fully ionized non-magnetic atmosphere, and the dotted line is for a blackbody with $T = 5 \times 10^{5}$ K.

models is due to the finite energy grid of the models and not an indication of the true line width; the true width is narrower.) It is clear from Fig. 4 that spectral features due to bound species at this field strength lie within the extreme UV ($E \gtrsim 50$ eV) to very soft X-ray ($E \lesssim 0.2$ keV) regime and therefore, are likely to be unobservable due to interstellar absorption. However, the effect of bound species on the temperature profile of the atmosphere and the continuum flux is significant. In particular, the optical flux is higher for the partially ionized atmospheres compared to the fully ionized atmospheres for the same $T_{\rm eff}$. On the other hand, the partially and fully ionized models both yield very similar (neglecting the spectral features) X-ray flux for a given effective temperature, with the partially ionized model fluxes slightly lower than those for the fully ionized models; thus fitting only the high energy flux with fully ionized models would yield fairly accurate NS temperatures.

Fig. 5 compares the partially and fully ionized models (neglecting vacuum polarization) of hydrogen atmospheres with $B = 5 \times 10^{14}$ G and $T_{\rm eff} = 5 \times 10^6$ K. Neglecting vacuum polarization allows us to distinguish features due to neutral atoms in the atmosphere; broad absorption features due to bound-free and bound–bound transitions at $E \sim 0.76$ and 4 keV, respectively, are apparent (the latter is from blending of two bound–bound transitions at 3.4 and 6.5 keV). The continuum flux between the models is not significantly different, and as noted in Ho and Lai (2001, 2003) and Zane et al., 2001), the proton cyclotron line is very broad when vacuum polarization is neglected. Fig. 6 compares the models with vacuum polarization (complete mode conversion; see Ho and Lai, 2003). We see that vacuum polarization softens the high energy tail of the spectrum in the partially ionized model, like the fully ionized model. In addition, we see that vacuum polarization also suppresses spectral features due to the bound species of hydrogen. The reduced width of the proton cyclotron line and spectral features associated with bound transitions makes these features difficult to observe with current X-ray detectors, and we suggest that the absence of lines in the observed spectra of several AXPs (Patel et al., 2001; Juett et al., 2002; Tiengo et al., 2002) may be an indication of the vacuum polarization effect at work in these systems.

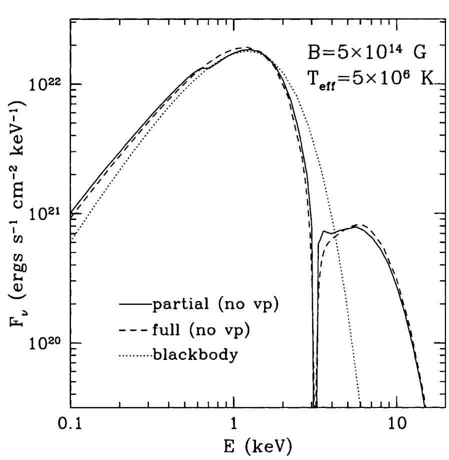

Fig. 5. Spectra of hydrogen atmospheres with $B = 5 \times 10^{14}$ G, $T_{\rm eff} = 5 \times 10^6$ K, and neglects vacuum polarization. The solid line is for a partially ionized atmosphere, the dashed line is for a fully ionized atmosphere, and the dotted line is for a blackbody with $T = 5 \times 10^6$ K.

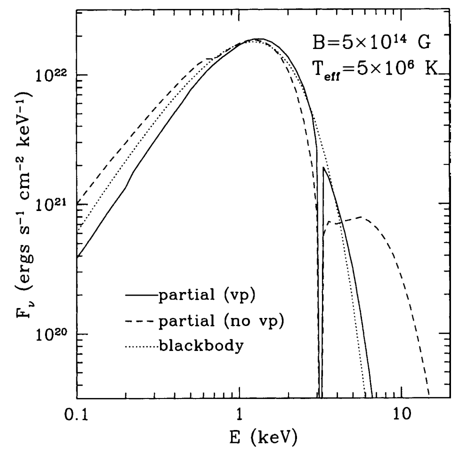

Fig. 6. Spectra of partially ionized hydrogen atmospheres with $B = 5 \times 10^{14}$ G and $T_{\rm eff} = 5 \times 10^6$ K. The solid line is for an atmosphere which includes vacuum polarization, the dashed line is for an atmosphere which neglects vacuum polarization, and the dotted line is for a blackbody with $T = 5 \times 10^6$ K.

Acknowledgements

We are grateful to the Cornell Hewitt Computer Laboratory for the use of their facilities. This work is supported in part by NASA Grant NAG 5-12034 and NSF Grant AST 9986740. D.L. is also supported by a fellowship from the A.P. Sloan Foundation. The work of A.Y.P. is supported by RFBR Grant 02-02-17668.

References

Becker, W. X-ray emission characteristics of pulsars, in: Martens, P.C.H., Tsuruta, S., Weber, M.A. (Eds.), Proceedings of the IAU Symposium 195, Highly Energetic Physical Processes and Mechanisms for Emission from Astrophysical Plasmas. Astronomical Society of the Pacific, San Francisco, pp. 49–60, 2000.

Bulik, T., Pavlov, G.G. Polarization modes in a strongly magnetized hydrogen gas. Astrophys. J. 469, 373–387, 1996.

Gnedin, Yu.N., Pavlov, G.G., Shibanov, Yu.A. Effect of vacuum birefringence in a magnetic field on the polarization and beaming of X-ray pulsars. Sov. Astron. Lett. 4, 117–119, 1978.

Ho, W.C.G., Lai, D. Atmospheres and spectra of strongly magnetized neutron stars. Man. Not. Roy. Astron. Soc. 327, 1081–1096, 2001.

Ho, W.C.G., Lai, D. Atmospheres and spectra of strongly magnetized neutron stars – II. The effect of vacuum polarization. Mon. Not. Roy. Astron. Soc. 338, 233–252, 2003.

Ho, W.C.G., Lai, D., Potekhin, A.Y., Chabrier, G. Atmospheres and spectra of strongly magnetized neutron stars – III. Partially ionized hydrogen models. Astrophys. J. 599, 1293–1301, 2003.

Hurley, K. 4.5 ± 0.5 soft gamma ray repeaters in review, in: Kippen, R.M., Mallozzi, R.S., Fishman, G.J. (Eds.), Gamma-Ray Bursts: Fifth Huntsville Symposium, AIP Conference Proceedings 526. American Institute of Physics, New York, pp. 515–522, 2000.

Israel, G., Mereghetti, S., Stella, L. Observations of anomalous X-ray pulsars. Memorie della Societá Astronomica Italiana 73, 465–476, 2002.

Juett, A.M., Marshall, H.L., Chakrabarty, D., Schulz, N.S. Chandra high-resolution spectrum of the anomalous X-ray pulsar 4U 0142 + 61. Astrophys. J. 568, L31–34, 2002.

Lai, D., Ho, W.C.G. Resonant conversion of photon modes due to vacuum polarization in a magnetized plasma: implications for X-ray emission from magnetars. Astrophys. J. 566, 373–377, 2002.

Lai, D., Ho, W.C.G. Transfer of polarized radiation in strongly magnetized plasmas and thermal emission from magnetars: effect of vacuum polarization. Astrophys. J. 588, 962–974, 2003.

Mereghetti, S., Chiarlone, L., Israel, G.L., Stella, L. Anomalous X-ray pulsars, in: Becker, W., Lesch, H., Trümper, J. (Eds.), Proceedings of the 270 WE-Heraeus Seminar on Neutron Stars, Pulsars, and Supernova Remnants. MPI, Garching, pp. 29–43, 2002.

Mihalas, D. Stellar Atmospheres, second ed. W.H. Freeman, San Francisco, 1978.

Patel, S.K., Kouveliotou, C., Woods, P.M., et al. Chandra observations of the anomalous X-ray pulsar IE 2259 + 586. Astrophys. J. 563, L45–48, 2001.

Pavlov, G.G., Gnedin, Yu.N. Vacuum polarization by a magnetic field and its astrophysical manifestations. Sov. Sci. Rev. E 3, 197–253, 1984.

Pavlov, G.G., Shibanov, Yu.A., Zavlin, V.E., Meyer, R.D. Neutron star atmospheres, in: Alpar, M.A., Kiziloglu, U., van Paradijs, J. (Eds.), Lives of the Neutron Stars. Kluwer Academic Press, Boston, pp. 71–90, 1995.

Pavlov, G.G., Zavlin, V.E., Sanwal, D. Thermal radiation from neutron stars: Chandra results, in: Becker, W., Lesch, H., Trümper, J. (Eds.), Proceedings of the 270 WE-Heraeus Seminar on Neutron Stars, Pulsars, and Supernova Remnants. MPI, Garching, pp. 273–286, 2002.

Potekhin, A.Y., Chabrier, G. Equation of state and opacities for hydrogen atmospheres of neutron stars with strong magnetic fields. Astrophys. J. 585, 955–974, 2003.

Thompson, C., Duncan, R.C. Soft gamma ray repeaters as very strongly magnetized neutron stars. II. Quiescent neutrino, X-ray, and Alfvén wave emission. Astrophys. J. 473, 322–342, 1996.

Thompson, C. Astrophysics of the soft gamma ray repeaters and anomalous X-ray pulsars, in: Kouveliotou, C., Ventura, J., van den Heuvel, E. (Eds.), Neutron Star-Black Hole Connection. Kluwer, Dordrecht, pp. 369–392, 2001.

Tiengo, A., Göhler, E., Staubert, R., Mereghetti, S. Anomalous X-ray pulsar IE 1048.1–5937: phase resolved spectroscopy with the XMM-Newton satellite. Astron. Astrophys. 383, 182–187, 2002.

Treves, A., Turolla, R., Zane, S., Colpi, M. Isolated neutron stars: accretors and coolers. Pub. Astron. Soc. Pacific. 112, 297–314, 2000.

Zane, S., Turolla, R., Stella, L., Treves, A. Proton cyclotron features in thermal spectra of ultramagnetized neutron stars. Astrophys. J. 560, 384–389, 2001.

Zavlin, V.E., Pavlov, G.G. Modeling neutron star atmospheres, in: Becker, W., Lesch, H., Trümper, J. (Eds.), Proceedings of the 270 WE-Heraeus Seminar on Neutron Stars, Pulsars, and Supernova Remnants. MPI, Garching, pp. 263–272, 2002.